Vol. 55: 1–15, 2012
doi: 10.3354/cr01116

CLIMATE RESEARCH
Clim Res

Published November 15

Synoptic classification of 2009–2010 precipitation events in the southern Appalachian Mountains, USA

Ginger M. Kelly[1,*], L. Baker Perry[1], Brett F. Taubman[2], Peter T. Soulé[1]

[1]Department of Geography & Planning, and [2]Department of Chemistry, Appalachian State University, Boone, North Carolina 28607, USA

ABSTRACT: Precipitation processes and patterns in the southern Appalachian Mountains (SAM) are highly complex and varied due to the considerable diversity of synoptic-scale circulation patterns and associated orographic effects. Whereas frontal activity associated with extratropical cyclones is responsible for a large fraction of the annual precipitation in the region, 500 hPa cutoff lows, tropical cyclones, non-frontal air mass thunderstorms, and moist SE or NW low-level flow also produce considerable precipitation. This paper classifies the synoptic patterns associated with precipitation in the SAM over the course of a 16 mo period in 2009 and 2010. Precipitation events were identified using National Weather Service cooperative observer, Community Collaborative Rain, Hail, and Snow (CoCoRaHS), and other selected automated meteorological stations across the region. A combination of manual and automated approaches was used to create a synoptic classification of precipitation events in the SAM. Antecedent upstream air trajectories provided information on moisture source regions and low-level flow. Warm season precipitation events were influenced by air masses originating over the Gulf of Mexico and the Atlantic Ocean. These events were characterized by short periods of high-intensity precipitation that was primarily convective in nature. Cool season precipitation was associated with a variety of frontal types, as well as non-frontal mechanisms, characterized by longer, wetter, low-intensity events. These events were largely influenced by air masses originating over the Gulf of Mexico and to the northwest of the study area. In both seasons, precipitation events associated with frontal activity produced greater amounts of precipitation per event when compared with non-frontal activity.

KEY WORDS: Synoptic classification · Precipitation · Southern Appalachian Mountains

1. INTRODUCTION

The hydroclimatology of mountain regions — particularly in the context of recreational development, climate variability, and climate change — remains poorly understood (De Jong et al. 2009). While precipitation is the fundamental input to the hydrologic system in headwater catchments, precipitation processes in mountains remain poorly characterized and continue to be plagued by limited observational networks (Barry 2008). Major gaps remain in our understanding of orographic precipitation, including that of both the physical processes and spatial patterns. In particular, the synoptic patterns and antecedent upstream air trajectories associated with precipitation events in mountains are not well understood, even though precipitation variability due to changes in atmospheric circulation has been linked to considerable hydrologic change in mountain regions (Kaser et al. 2004, Francou et al. 2003). Projections of future climate variability and change in mountainous regions must incorporate the effect of projected changes in atmospheric circulation on precipitation patterns. In this study we create a synoptic classification scheme that links precipitation patterns to the synoptic-scale atmospheric circulation and associated frontal boundaries, over a 16 mo period in 2009 to 2010. We also investigate precipitation patterns in opposing phases of

*Email: kellygm@email.appstate.edu

El Niño Southern Oscillation (ENSO; i.e. El Niño and La Niña) and during an extremely negative phase of the Arctic Oscillation (AO), thereby providing an important context for how precipitation characteristics may respond to future changes in atmospheric circulation (e.g. Li et al. 2010). Lastly, this paper also introduces a synoptic classification scheme created for 2009–2010 precipitation events that may have broad application in other mid-latitude mountain regions.

The southern Appalachian Mountains (SAM) of the southeastern US (SEUS) are characterized by considerable topographic variability, exerting influence on the distribution and intensity of precipitation across the region (Konrad 1996, Barros & Kuligowski 1998, Perry & Konrad 2006). Mean annual precipitation ranges from ~900 mm in the heavily shadowed valleys to nearly 2500 mm on ridges highly exposed to moisture transport from the Atlantic Ocean and Gulf of Mexico. Synoptic-scale circulation patterns associated with precipitation events are quite diverse on both inter- and intra-seasonal timescales. In the warm season, precipitation is closely linked to the westward extent and strength of the Bermuda High (e.g. Li et al. 2010) while cool season precipitation is primarily tied to the track and frequency of extratropical cyclones and associated frontal activity (Cortinas et al. 2004). Frontal boundaries, though most common in the cool season, are present throughout the year and contribute necessary components for the formation of precipitation.

West-northwest winds dominate in the cool season, while warm, moist air is carried to the region from the Gulf of Mexico and Atlantic Ocean in the warm season. The northeast-southwest orientation of the SAM favors orographic precipitation in association with low-level southeast and northwest flow. In the cool season, low-level upslope flow is predominantly northwesterly, resulting in orographically enhanced northwest flow snowfall (NWFS) with a periodic Great Lakes connection (Perry et al. 2007). Southeast upslope flow precipitation is more prevalent during the warm season (Lee & Goodge 1984, Johnstone & Burrus 1998), but can also occur in the cool season. In the Appalachian region, the majority of heavy rainfall events, defined as those producing at least 50 mm of measurable precipitation, occur during the warm season (Konrad & Meentemeyer 1994). In the cool season, NWFS accounts for nearly 50% of annual average snowfall (Perry et al. 2007).

Regional influences of topography (Konrad 1996, Perry & Konrad 2006) and atmospheric aerosols (Rosenfeld 1999, Givati & Rosenfeld 2004, Lohmann & Feichter 2005, Jirak & Cotton 2006, Rosenfeld et al. 2007) combined with the limited availability of precipitation observations (both temporally and spatially) add to the difficulty of understanding patterns of precipitation in the SAM. Heavy rainfall and rapid snowmelt have led to disastrous flooding in the region (Barros and Lettenmaier 1994, Lapenta et al. 1995, Barros & Kuligowski 1998, Gaffin & Hotz 2000, Lecce 2000, Graybeal & Leathers 2006), and drought conditions have caused hundreds of millions of dollars in damages and resource losses (Maxwell & Soulé 2009). Climate models suggest that the SEUS may become drier and warmer in the coming decades while experiencing more intense periods of deluge and drought, particularly as a result of anthropogenic-induced warming (Lynn et al. 2007, Karl et al. 2009, Li et al. 2010); however many global circulation models do not effectively account for the topographic influences on precipitation or the direct and indirect effects of aerosols (Power et al. 2006). An understanding of current synoptic influences of precipitation in the SAM is critical in order to assess how possible changes in atmospheric circulation patterns at a variety of scales may ultimately impact the frequency and intensity of precipitation events.

A major goal of this study is to create a synoptic classification scheme for precipitation events during 2009 to 2010 in the SAM, thereby achieving a greater understanding of the synoptic influences on precipitation processes in the region and ultimately better informing regional weather forecasting and modeling of future climate scenarios. While spanning only 16 mo, the study period included both warm and cool phase ENSO events, allowing for an examination of the dominant synoptic types of precipitation favored during each phase for this particular time period. In the SEUS, warm-phase ENSO typically results in positive precipitation anomalies during the winter and negative anomalies during the summer, with the opposite being true for the cool-phase ENSO. Similarly, in the SAM, precipitation anomalies during summer months tend to be positive during cool-phase ENSO (Barlow et al. 2001, Mo & Schemm 2008), with a strong relationship existing between winter and early spring precipitation and ENSO in Boone, North Carolina. The synoptic classification scheme presented in this paper also provides a framework for the analysis of aerosol-precipitation interactions in the SAM (e.g. Kelly et al. 2012), adding to our understanding of the reciprocal relationship between aerosols and climate (e.g. Power et al. 2006) in the SAM. Additionally, west-to-east precipitation indices reveal the orographic effects of precipitation in the SAM,

wherein considerable spatial variability can occur between the North Carolina-Tennessee border and the Blue Ridge Escarpment, particularly during cool season non-frontal precipitation events.

Synoptic climatologies have been created to classify precipitation in the SEUS and the SAM (Table 1). Konrad (1997) determined that heavy precipitation events are tied to the advection of warm, moist air and identified 5 synoptic patterns in the SEUS. These patterns included descriptions of boundary layer and low-level convergence scenarios within the synoptic-scale vicinity of heavy rainfall. Keim (1996) also analyzed the synoptic properties associated with seasonal heavy rainfall events in the SEUS based on a scheme adopted from Muller (1977) wherein events are classified as frontal, tropical disturbance, or air mass. The resulting classification revealed that most seasonal heavy rainfall across the region is associated with frontal systems. Diem (2006) examined the synoptic controls of both wet and dry periods in the Atlanta, Georgia metropolitan area, identifying the impact of varying synoptic-scale circulation patterns on precipitation. Wet periods were identified in association with upper-level troughs in the interior SEUS coupled with high pressure along the eastern coast; dry periods were associated with interior anticyclones coupled with low pressure along the SEUS coast.

Konrad & Meentemeyer (1994) examined synoptic controls of warm season heavy rainfall focusing on the Appalachian region. Synoptic classification was based on the orientation and location of lower tropospheric warm air advection, with which 60% of study events were associated. Focusing on the Great Smoky Mountains in the SAM, Perry et al. (2010) manually classified snowfall events that took place over a 14 yr time period, based on surface and 500-hPa synoptic patterns. This resulted in 13 synoptic classes similar to those described by Miller (1946), including Miller A cyclones, which account for the greatest contribution of annual snowfall across the region and are associated with northwest flow at their heaviest. To further address cold season precipitation patterns, Perry et al. (2007) used backward air trajectory analyses to create a synoptic classification of NWFS events impacting the SAM. NWFS events can account for roughly 50% of annual snowfall along windward slopes in the SAM and are often associated with a Great Lakes connection.

The hybrid classification scheme created in this study was based on 16 mo of precipitation events classified as either frontal or non-frontal precipitation, with various sub-types (Fig. 1). A manual scheme was used to accurately assess and categorize those aspects of the synoptic-scale circulation that were tied to the precipitation development. In addition, we also use 2 automated approaches to classifying precipitation events: low-level wind directions by quadrant (e.g. NE, SE, SW, and NW) from Beech Mountain (1806 m above sea level [a.s.l.]) and statistical clustering of antecedent upstream air trajectories. Automatic classification schemes alone can be useful for air mass typing (e.g. Sheridan 2002), but the combination of manual and automated ap-

Table 1. Previous work on the synoptic classification of precipitation in the Southeastern United States (SEUS) and the southern Appalachian Mountains (SAM)

Region	Precipitation focus	Classifications	Source
SEUS	Heavy rainfall	Pacific high, continental high, frontal overrunning, coastal return, gulf return, frontal gulf return, gulf tropical disturbance, gulf high	Muller (1977)
Warm season heavy rainfall	SAM	Location and orientation of lower tropospheric warm air advection	Konrad & Meentemeyer (1994)
SEUS	Heavy rainfall	Frontal, tropical disturbance, air mass	Keim (1996)
SEUS	Heavy rainfall	5 patterns based on boundary layer characteristics and low-level convergence scenarios	Konrad (1997)
Atlanta/metropolitan area, Georgia	Wet/dry periods	Wet periods associated with upper-level troughs in interior SEUS coupled with high pressure along the coast; dry periods associated with interior anticyclones coupled with low pressure along the coast	Diem (2006)
SAM	Northwest flow snowfall	5 classes of air trajectories associated with northwest flow snowfall	Perry et al. (2007)
SAM	Snowfall	12 synoptic types based on daily surface and 500 hPa analyses	Perry et al. (2010)

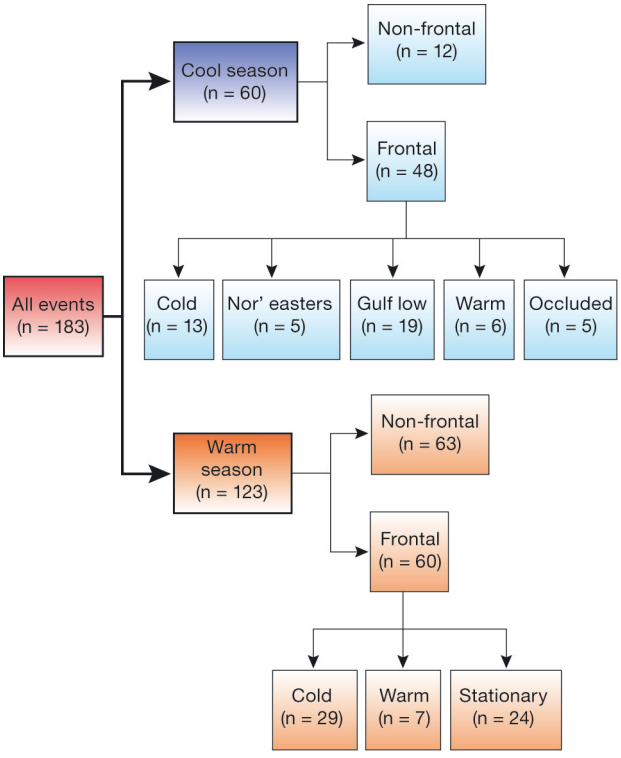

Fig. 1. Synoptic Classification Scheme

proaches used in this study is helpful in identifying key synoptic patterns (particularly related to fronts) associated with precipitation events.

In addition to creating a synoptic classification scheme for precipitation events in the SAM, the following research questions guided this study: (1) Which synoptic patterns are associated with 2009–2010 precipitation events across the SAM and how they vary between warm and cool season? (2) How do precipitation totals and intensity vary by synoptic class and antecedent upstream air trajectories during 2009–2010?

2. DATA AND METHODS

2.1. Research setting

The study area was centered on the Appalachian Atmospheric Interdisciplinary Research (AppalAIR) facility (36.213° N, 81.691° W, 1076 m a.s.l.) on the campus of Appalachian State University in Boone (Fig. 2). AppalAIR is an air quality and climate research station, which includes a 30 m tower for continuous atmospheric monitoring and a suite of meteorological and aerosol instrumentation (e.g. Kelly et al. 2012). The AppalAIR facility is located near the crest of the SAM and is therefore highly exposed to air masses from all directions.

Daily precipitation totals at climate monitoring stations within the study area were analyzed during the period 01 June–30 September in 2009 and 2010 (i.e. warm seasons) and 01 November 2009–30 April 2010 (i.e. cool season) (Fig. 2). Warm season and cool season events were separated due to the spatial and temporal variability in the stability, precipitation development, and biogenic and anthropogenic aerosol emissions that characterize each season. The shoulder months of May and October were omitted from this study to provide a distinct separation of warm and cool season events. These transitional months encompass the change in weather systems, phenological cycles, and aerosol properties that accompany the change of seasons in the SAM.

2.2. Active study period

The 16 mo time period examined in this study included a variety of circulation regimes, weather patterns, and precipitation event types that are characteristic of and likely to impact the SAM. Although not a synoptic climatology, due to the short duration of the study period, the results of the synoptic classification are nonetheless helpful in understanding the variety of precipitation event types (and associated spatial patterns) that affect the region, particularly in the context of anomalous atmospheric circulation.

The warm (2009–2010) and cold (2010–2011) phases of ENSO and a highly negative AO (winter [DJF] 2009–2010) coupled with persistent 500 hPa ridge during summer (JJA) 2010 resulted in near normal temperatures, but above normal precipitation (limited to 2009) during the study period (June 2009 to September 2010). The climatological summer of 2009 (JJA), as well as the following winter (DJF 2009–2010) were characterized by lower temperatures and higher precipitation than normal on the western slopes of the SAM. During the month of July 2009, daily high temperatures in Boone exhibited an average departure of −1.4°C from the 1929–2009 mean. These negative departures were related to a persistent 500 hPa trough over the eastern US, resulting in frequent shower activity. The National Weather Service (NWS) cooperative observer (COOP) station in Boone reported a higher number of days of observed precipitation, with 14 more days during the first warm season and 7 more days during the cool season, compared to 1929–2009 normals.

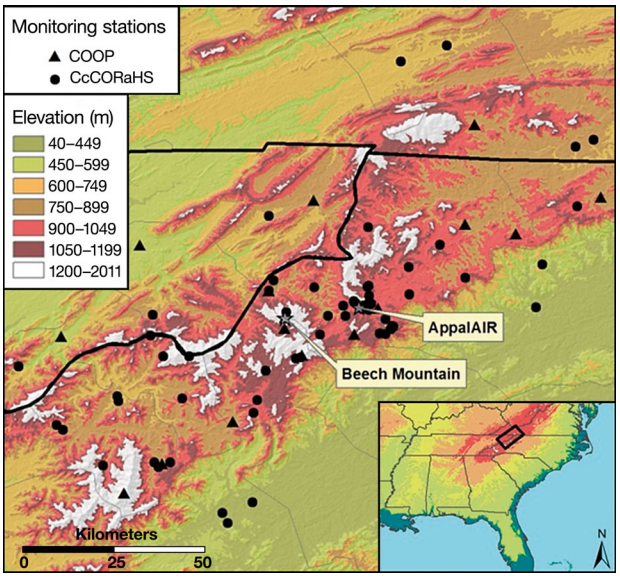

Fig. 2. Topography of study area, including locations of the Appalachian Atmospheric Interdisciplinary Research (AppalAIR) facility, Beech Mountain, and all National Weather Service cooperative observer (COOP) network and Community Collaborative Rain, Hail, and Snow (CoCoRaHS) monitoring stations

Throughout the severe winter season, many stations across the region set records for total snowfall and days of snow cover (Perry et al. 2010), as this was the most severe winter in the SAM since the 1970s. In contrast, JJA 2010 was characterized by much higher temperatures and drier conditions. Ultimately, temperatures averaged close to normal for the period of study, while precipitation was considerably above normal, making this an ideal period to analyze synoptic patterns associated with precipitation events in the SAM.

2.3. Precipitation data and event identification

Periods of precipitation were identified from the Boone Automated Weather Observing System (AWOS) hourly weather-type data and corroborated with hourly precipitation data from the Boone Environmental and Climate Observing Network (ECO Net) station and daily precipitation totals from the Boone COOP station and the CoCoRaHS network stations (Cifelli et al. 2005) in the town of Boone. Events that qualified for this study produced measurable precipitation (≥0.25 mm) at one or more of the aforementioned monitoring stations. Events were separated from one another by ≥6 h of no reported precipitation. Starting, ending, and maturation times for each event were identified based on Boone AWOS hourly weather-type data, an approach consistent with that of Perry et al. (2007, 2010) in their investigations of snowfall in the SAM. The beginning of an event was defined as the hour corresponding with the first report of precipitation of any kind, with a minimum of 6 h of no precipitation beforehand; the maturation of an event was defined as the hour corresponding with the heaviest precipitation reports; and the ending of an event was defined as the hour corresponding with the last report of precipitation of any kind during the event. Precipitation data were obtained and compiled for analysis from 59 monitoring stations in the CoCoRaHS network and from 16 monitoring stations in the COOP network located above 305 m elevation (Fig. 2).

2.4. Synoptic classification

Events were classified using a new synoptic classification scheme, adapted from Keim (1996) (Fig. 1). After being classified by season (e.g. warm and cool), events were classified as frontal or non-frontal events, based on archived 3 hourly National Centers for Environmental Prediction (NCEP) Service Records Retention System (SRRS) Analysis and Forecast Charts (NCEP 2010a) and NCEP daily weather maps (NCEP 2010b). Frontal and non-frontal precipitation events were differentiated by the synoptic influences driving these events. Frontal events were identified by the presence of a frontal boundary or surface low pressure, while non-frontal events included convective and orographic processes in the absence of identifiable frontal mechanisms.

Previous studies have employed distance criteria ranging from 100 to 2500 km from the area of interest in order to classify various frontal events taking place in lowland areas (Muller 1977, Harnack et al. 2001) and also in mountainous terrain (Maddox et al. 1979, Konrad & Meentemeyer 1994, Konrad 1997, Lin et al. 2001). In the cross-front direction, the spatial scale of frontal zones is typically on the order of 100 km (Lackmann 2011). In this study, frontal events were identified by the presence of a frontal boundary within 300 km of the study area at the time of event maturation, as this distance consistently accounted for pre-frontal precipitation as a result of the moistening and strengthening of upslope flow. Fronts can be tied to isentropic lift, moist low-level flow, and a surface/upper air boundary that can result in the development of orographic precipitation or serve as a trigger for convection to develop and propagate into

the region. Frontal events were further classified as cold, warm, stationary, or occluded based on SRRS and NCEP weather charts. In the absence of a clear frontal boundary within 300 km of the study area, events were classified as Gulf Lows when precipitation was associated with a low pressure center in the Gulf of Mexico and classified as Nor'easters if precipitation was associated with a surface cyclone tracking to the northeast. Nor'easters were sometimes associated with a 500 hPa low passing nearby the study area or overhead. Non-frontal events were defined as precipitation occurring with no discernible front within 300 km from the study area.

Precipitation events were also classified based on low-level wind directions and statistical clustering of antecedent upstream air trajectories. Events were further classified based on spatial coverage, with scattered events constituting <75% of active stations reporting measureable precipitation and widespread events ≥75% of active stations reporting measureable precipitation. Additionally, events were analyzed according to upper and lower quartile precipitation values, creating subcategories of events representing heavy and light precipitation, respectively. Daily mean composite plots were created for individual events/groups of similar events illustrating atmospheric variables, including geopotential height at 500 hPa and sea level pressure (NCEP 2010c). Composite plots were created using the NCEP/National Center for Atmospheric Research (NCAR) reanalysis dataset (Kalnay et al. 1996). Additionally, west-to-east precipitation indices were created for each event type revealing the orographic effects on the spatial variability of precipitation during the study period in the SAM.

2.5. Meteorological data

Meteorological data were collected from the Beech Mountain monitoring station (BEECHTOP; 36.185° N, 81.881° W; 1678 m a.s.l.), located ~17.4 km west of AppalAIR (Fig. 2). Average temperature, relative humidity, wind speed, and wind direction values were compiled for beginning and maturation hour of each event and summarized by event type. Average wind direction values were calculated as unit-vector averages, and most frequent wind directions were determined by analysis of a histogram of observed wind directions during each event. In contrast to Boone and other valley or ridge-top locations, wind direction at Beech Mountain is not considerably controlled by local topography, and data from this location are therefore broadly representative of lower tropospheric (~825 hPa) meteorological conditions. Meteorological data from BEECHTOP were not available from 26 December 2009 through 10 January 2010 due to severe ice and wind causing a catastrophic tower collapse.

Hour- and minute-resolution precipitation intensity values collected by an OTT Pluvio^2 weighing precipitation gauge were obtained from the NWS COOP station on Poga Mountain (36.253° N, 81.917° W; 1140 m a.s.l.) for events taking place November 2009 to September 2010. Precipitation intensity values (mm h^{-1}) were calculated for each event using precipitation totals from all COOP and CoCoRaHS stations as well as from the Boone ECONet station.

2.6. Trajectory analysis

The National Oceanic and Atmospheric Administration (NOAA) HYbrid Single Particle Lagrangian Integrated Trajectory (HYSPLIT) model, version 4 (Draxler & Rolph 2011), and 40 km Eta Data Assimilation System (EDAS) 3-hourly archive data were used to create 72 h, 3D kinematic backward air trajectories ending at maturation time of each event at the coordinate location of AppalAIR. Trajectories provide information on moisture and aerosol source regions influencing precipitation events in the SAM. To account for seasonal surface–atmosphere interactions in the lower troposphere at ~800 hPa, warm and cool season trajectories were run at 2000 and 1500 m a.s.l., respectively.

For each synoptic class (Fig. 1), a cluster analysis was performed on the backward air trajectories associated with the maturation hour of each precipitation event, an approach based on the clustering methodology used by Taubman et al. (2006). HYSPLIT uses multiple iterations to create clusters of trajectories by calculating the total spatial variance (TSV) among trajectories. In the first iteration, TSV is zero and each trajectory is considered a stand-alone cluster at this stage (i.e. N trajectories = N clusters) (Draxler 1999). Two trajectories are paired and the cluster spatial variance (SPVAR) is calculated, which is the sum of the squared distances between the endpoints of the paired clusters. TSV is then calculated, which is the sum of all cluster SPVARs, and pairs of clusters that are combined are those with the lowest increase in TSV. For the second iteration, the number of clusters is N – 1 since 2 trajectories were clustered together in the first iteration, resulting in one less stand-alone cluster. The same calculations and com-

parisons are performed, resulting in the combination of the 2 clusters with the lowest increase in TSV. Iterations continue until the very last 2 clusters are combined. After several iterations during the cluster analysis, TSV increases rapidly, indicating that trajectories being combined within the same cluster are not very similar. At this stage, clustering should stop. In a plot of TSV versus number of clusters, the step just before the large increase in TSV indicates the final number of clusters. While some subjectivity was involved in the choice of final number of clusters, a large change in TSV was required and the choice was not arbitrary.

2.7. Statistical tests

All datasets were tested for normality ($\alpha = 0.05$) using the Kolmogorov-Smirnov test. For data that were not normally distributed, differences of means were tested ($\alpha = 0.05$) using the Mann-Whitney *U* 2-sample rank sums test (non-parametric). When normally distributed, an independent samples *t*-test (parametric) was used. Differences of means of meteorological and precipitation values were tested for each event type, and comparisons were made between seasons, and also among different event types within the same season. One-way ANOVA analysis was used to determine the differences among frontal types within each season in terms of average precipitation and precipitation intensity.

3. RESULTS AND DISCUSSION

3.1. Warm season

While there were no significant differences in average total precipitation per event between each season, there were differences among synoptic types (Table 2). This study examined 2 warm seasons, resulting in 123 warm season precipitation events, of which 21% took place during June, 28% during July, 32% during August, and 20% during September. Warm season precipitation was associated with cold, warm, and stationary fronts as well as non-frontal mechanisms involving shallow upslope flow and terrain-induced convection. Warm season precipitation associated with frontal mechanisms produced significantly higher precipitation values than frontal precipitation during the cool season (Table 2). Warm season precipitation events lasted an average of 5 h, ranging in duration from 1 to 29 h, and displayed considerable variance in amount and intensity of measured precipitation (Table 3).

Warm season events were characterized by the presence of the North Atlantic Subtropical High (NASH) to the east (e.g. Li et al. 2010), which favored precipitation in the SEUS by the advection of moisture from the Atlantic Ocean and the Gulf of Mexico and resulted in dominant wind directions from the south and northwest (Table 2). During the warm season, the majority of air masses had a Gulf or Atlantic Ocean coastal connection and therefore higher moisture flux (Fig. 3A).

Nearly half of all warm season precipitation events were associated with frontal mechanisms and were characterized by short, intense precipitation (Table 4), although there was no significant difference in average total precipitation per event during warm season frontal and non-frontal precipitation events (Table 2). Warm season frontal events in this study were typically characterized by lower pressures in the study region and the presence of the NASH offshore to the east causing moist air advection from coastal regions. While warm season stationary fronts produced the greatest average total precipitation, there were no statistically significant differences in precipitation among warm season cold, warm, and stationary fronts. The greatest precipitation intensity was associated with non-frontal events during the warm season in this study (Table 3).

Cold fronts were responsible for 48% of all frontal precipitation events in the warm season. These events were associated with antecedent air that originated to the west and southwest (Fig. 4A) and with moisture advection from the Gulf of Mexico. Warm fronts accounted for 12% of warm season frontal precipitation events, and were associated with warm air advection from the south and southeast. Due to isentropic lifting, these events were typically widespread across the study area and approached from the west, with a few air masses originating from coastal areas (Fig. 4B). These events were also typically warmer at BEECHTOP during maturation (Table 4). Throughout the study region, precipitation associated with warm season warm fronts was typically the least intense and least productive of any warm season precipitation event type (Table 3).

Stationary fronts accounted for 40% of warm season frontal precipitation events and produced the highest average precipitation per event (Table 4). These events were generally widespread and originated either northwest of the study area or from the Gulf of Mexico, with a few cases that originated northeast of the study area and approached from the

Table 2. Summaries and mean differences of meteorological values at maturation for different precipitation events. Average total precipitation values are from National Weather Service cooperative observer (COOP) and Community Collaborative Rain, Hail, and Snow (CoCoRaHS) stations in study area. Average temperature, relative humidity, wind speed, and wind direction are from the Beech Mountain (BEECHTOP) meteorological station. p-values (2-tailed) **in bold**: significance at ≥95% CI. *Values obtained using parametric test

	Mean total precipitation	Temperature (°C)	Relative humidity (%)	Wind speed (m s^{-1})	Wind direction (°)	Most frequent wind direction(s)	Average spatial coverage (%)
Summary							
All events							
Warm (n = 123)	8.9	15.3	96.2	3.7	WSW (244)	S, NW	80
Cool (n = 60)	13.4	–2.2	98.8	5.7	S (176)	SSE, NW	69
Abs_diff	4.5	17.5	2.6	2.1			
p-value	0.919	**<0.001***	0.205	**0.004**			
Warm season							
Frontal (n = 60)	10.2	14.9	97.6	3.8	W (271)	W	82
Non-frontal (n = 63)	7.6	15.7	94.9	3.5	SW (220)	SSE, NW	78
Abs_diff	2.6	0.8	2.7	0.4			
p-value	0.231	0.110*	0.071	0.256*			
Cool season							
Frontal (n = 49)	15.8	–0.7	99.3	6.2	S (176)	SSE, WNW	73
Non-frontal (n = 12)	3.6	–8.0	97.0	3.6	WNW (302)	NW	52
Abs_Diff	12.2	7.3	2.3	2.6			
p-value	**0.007**	**0.003**	**0.013**	0.076*			
Difference							
Frontal							
Warm (n = 60)	10.2	14.9	97.6	3.8	W (271)	W	82
Cool (n = 48)	15.8	–0.7	99.3	6.2	S (176)	SSE, WNW	73
Abs_diff	5.6	15.6	1.7	2.4			
p-value	0.579	**<0.001**	0.391	**0.002***			
Non-frontal							
Warm (n = 63)	7.6	15.7	94.9	3.5	SW (220)	SSE, NW	78
Cool (n = 12)	3.6	–8.0	97.0	3.6	WNW (302)	NW	52
Abs_diff	4.0	23.7	2.1	0.1			
p-value	**0.010**	**<0.001***	0.773	0.917*			

Table 3. Precipitation intensity values. Data were collected from National Weather Service (NWS) cooperative observer (COOP), Community Collaborative Rain, Hail, and Snow (CoCoRaHS), Poga Mountain, and Boone Environmental and Climate Observing Network (ECONet) monitoring stations

	COOP/CoCoRaHS	Poga Mountain				ECONet	
	Regional mean	Hourly		Minute		Hourly	
	(mm h^{-1})	Max. (mm)	Mean (mm)	Max. (mm)	Mean (mm)	Max. (mm)	Mean (mm)
All events							
Warm season	2.46	16.79	0.73	2.79	0.01	26.20	0.43
Cool season	0.90	15.09	0.51	0.61	0.01	20.80	0.42
Warm season							
All frontal	2.79	12.90	0.84	1.91	0.013	8.60	0.38
Cold front	3.60	7.59	0.92	1.09	0.015	4.30	0.19
Warm front	1.38	3.00	0.51	0.20	0.008	3.60	0.26
Stationary front	2.23	12.90	0.89	1.91	0.013	8.60	0.55
Non-frontal	2.14	16.79	0.56	2.79	0.007	26.20	0.48
Cool season							
All frontal	1.00	15.09	0.61	0.61	0.011	20.80	0.53
Cold front	1.07	7.70	0.88	0.20	0.011	1.00	0.08
Warm front	1.31	4.90	0.55	0.61	0.011	9.70	0.78
Occluded front	1.67	15.09	1.01	0.20	0.002	19.80	1.42
Gulf lows	0.87	5.99	0.61	0.20	0.013	20.80	0.52
Nor'easters	0.29	2.01	0.18	0.20	0.002	0.30	0.02
Non-frontal	0.48	1.50	0.09	0.102	0.0006	1.00	0.01

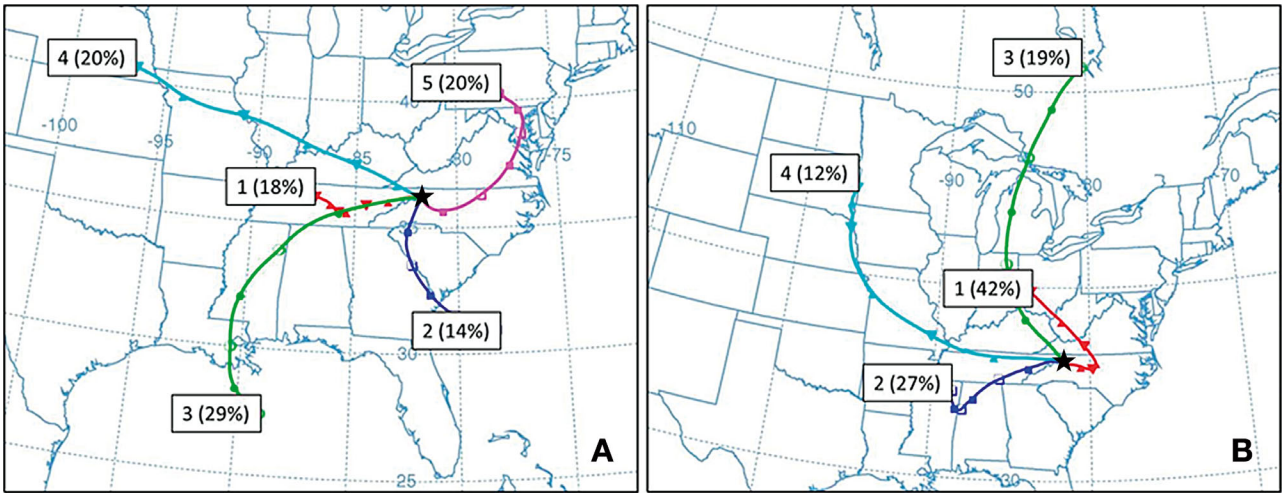

Fig. 3. Hybrid single particle Lagrangian integrated trajectory cluster analysis of backward air trajectories representing maturation hour of each precipitation event during (A) warm season (123 backward trajectories [BTs]) and (B) cool season (59 BTs) created using 40 km Eta Data Assimilation System 3-hourly archive data. (★) Source at 36.21° N, 81.69° W. Cluster mean trajectories are represented by the colored lines. Parentheses: % of air BTs in each cluster. BTs terminating before 72 h, likely as a result of missing meteorological data, were not included in the clustering

southeast (Fig. 4C). The study area was most often in the cold sector of the frontal boundary at maturation, resulting in higher precipitation totals possibly tied to isentropic lift associated with lower-tropospheric warm air advection or elevated convection over a stable surface layer.

Non-frontal events constituted ~51% of warm season precipitation events in this study. In very few cases (n = 3), precipitation was tied to a 500 hPa low pressure passing directly over the study area, but this pattern was not common enough to warrant a standalone analysis and was thus grouped with warm season non-frontal precipitation events. Non-frontal precipitation during the warm season likely occurred in association with local convective and orographic processes, such as described by Barros & Kuligowski (1998). Conditions for the development of precipitation can be enhanced through orographic processes such as forced lifting and differential advection of moist air. A large percentage (59%) of events exhibited westerly flow at the study area, half of which were associated with moisture that likely originated in the Gulf of Mexico (Fig. 4D). Approximately 67% of warm season non-frontal precipitation events were widespread across the study area, while the remaining 33% were scattered. Overall, precipitation events in this category were associated with strong areas of low pressure to the west and north of the study area and the presence of the NASH offshore to the east, causing the advection of warm, moist air from the Atlantic Ocean and the Gulf of Mexico. These events were also characterized by the presence of a slight trough in 500 hPa heights near the study area, indicative of the presence of cool, moist air. Across the region, warm season non-frontal precipitation events produced some of the most intense maximum minute and hourly precipitation intensities of all warm season precipitation events, likely due to the higher moisture content and somewhat slower storm movement.

West-to-east precipitation indices reveal an inconsistent pattern of the spatial variability of precipitation associated with warm season precipitation events (Table 5). Weaker flow and the dominance of convective precipitation during the warm season resulted in greater spatial variability and less windward-leeward contrasts. One-way ANOVA analysis results indicated no statistically significant differences in average precipitation among warm season frontal types (Levene = 0.004; Welch = 0.139) or cluster groups (Levene = 0.016; Welch = 0.577).

3.2. Cool season

This study examined one cool season, composed of 60 precipitation events, of which roughly 7% took place in November, 13% in December, 27% in January, 22% in February, 20% in March, and 13% in April. Cool season precipitation was associated with cold, warm, and occluded fronts as well as Gulf lows and Nor'easters. There were no stationary fronts

Table 4. Summary of warm season precipitation event types. Average total precipitation values from National Weather Service cooperative observer (COOP) and Community Collaborative Rain, Hail, and Snow (CoCoRaHS) stations in the study area. Average temperature, relative humidity, wind speed, and wind direction are from the Beech Mountain (BEECHTOP) meteorological station. Significance: Levene = 0.004; Welch = 0.139

Event types	n	Mean spatial coverage (%)	Mean duration (range) (h)	Mean total precipitation (mm)	Temperature (°C)	Relative humidity (%)	Wind speed ($m\ s^{-1}$)	Wind direction (°)	Most frequent wind direction(s)	Monthly distribution (%)			
										J	J	A	S
All frontal	60	82	5 (1–22)	10.2	14.9	97.6	3.8	W (271)	WNW	23	33	25	18
Cold front	29	76	4 (1–17)	8.5	14.7	97.6	3.9	WNW (288)	W	21	24	28	28
Warm front	7	91	4 (1–9)	5.3	16.0	98.5	3.5	SW (220)	S, NW	43	57		
Stationary front	24	88	7 (1–22)	13.6	14.8	97.3	3.8	SW (232)	NW	21	38	29	13
Non-frontal	63	78	5 (1–29)	7.6	15.7	94.9	3.5	SSW (207)	SSE, NW	19	22	38	21

Table 5. Standardized precipitation index values for precipitation events during warm and cool seasons by synoptic type and backward air trajectory. Indices represent a standardized ratio of precipitation from west-to-east using precipitation event totals from Erwin and Elizabethton, Tennessee (Northeast) combined with 2 Wilkes County, North Carolina, CoCoRaHS stations. Positive values: more precipitation on northwestern slopes; Negative values: greater precipitation on southeastern slopes. NA: not available

Event type	Warm season	Cool season
All events	0.13	0.04
Non-frontal	0.1	0.98
All frontal	0.15	−0.1
Cold fronts	0.21	0.51
Warm fronts	0.08	−0.28
Occluded fronts	NA	−0.64
Stationary fronts	0.09	NA
Gulf lows	NA	−0.34
Nor'easters	NA	0.31
Cluster 0	NA	−0.24
Cluster 1	−0.21	−0.35
Cluster 2	0.36	0.36
Cluster 3	0.3	0.53
Cluster 4	0.09	0.62
Cluster 5	−0.03	NA

associated with precipitation in the cool season. Non-frontal mechanisms, such as northwest upslope flow (e.g. Perry et al. 2007) were also responsible for some events. Cool season precipitation events exhibited an overall longer duration than warm season events, lasting an average of 16 h and ranging in duration from 1 to 66 h. Across the region, cool season precipitation events exhibited generally lower precipitation intensities than warm season events (Table 3).

Cool season precipitation events were associated with lower pressures over the study area and to the northeast, and with higher pressures to the west, suggesting the advection of air from inland areas and much less moisture originating in the Gulf of Mexico or the Atlantic Ocean. Most air masses associated with cool season precipitation events originated southwest of the study area or in the Midwest and approached the study area from the west and southeast (Fig. 3). Approximately 52% of all cool season precipitation events were snow events. At Poga Mountain, 229 cm of snowfall (158 mm liquid equivalent) occurred during the cool season, representing 25% of total cool season precipitation.

Cool season precipitation events, particularly those associated with frontal mechanisms, exhibited significantly higher wind speeds than warm season precipitation events (Table 2). The vast majority (80%) of cool season precipitation events were associated with

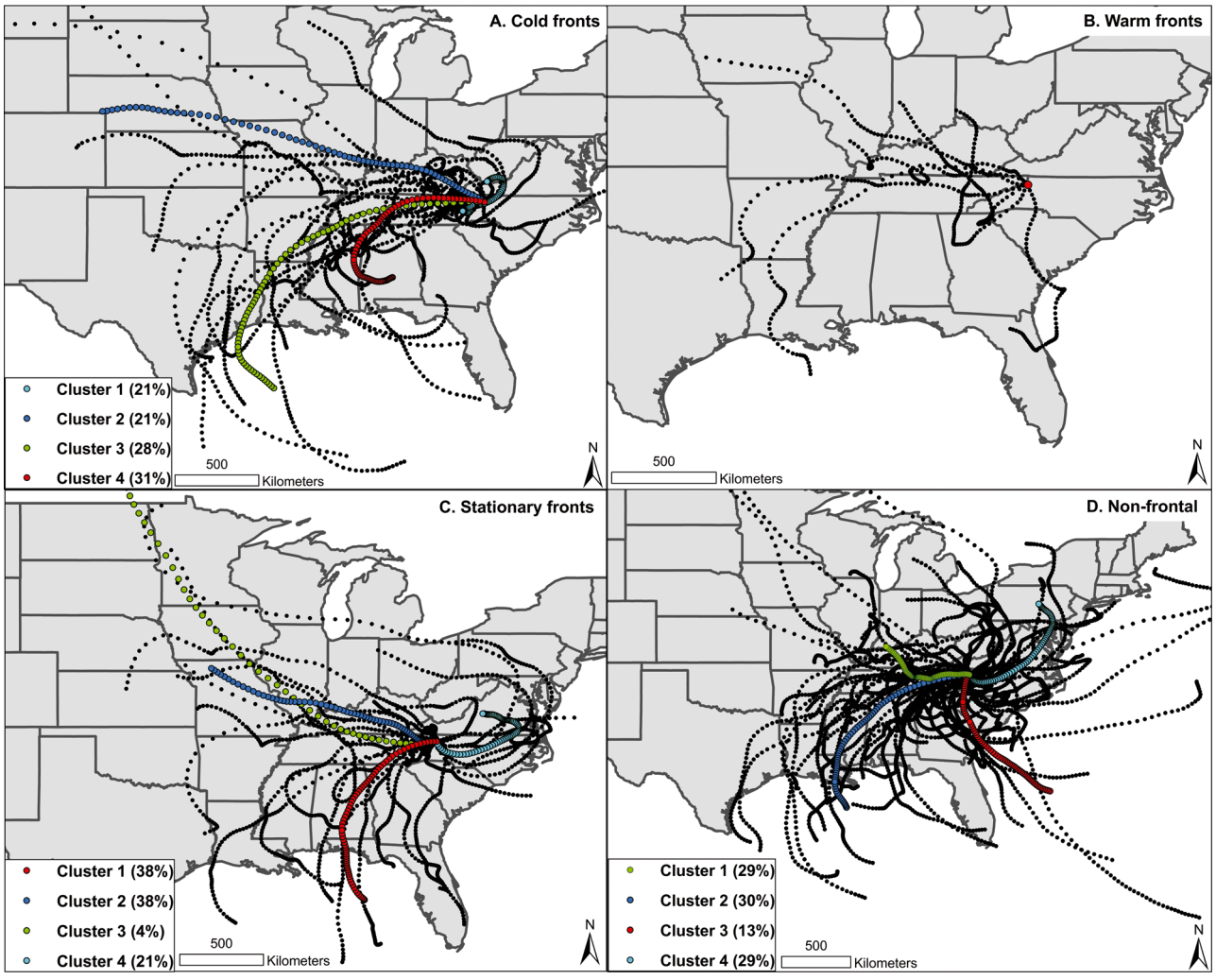

Fig. 4. Backward air trajectories representing maturation hour of each warm season precipitation event. Plots represent precipitation associated with (A) cold fronts, (B) warm fronts, (C) stationary fronts, and (D) non-frontal events. HYSPLIT cluster mean trajectories are in color where applicable; clusters are numbered. An insufficient number of backward air trajectories prevented HYSPLIT cluster analysis in the case of warm season warm fronts: individual trajectories are plotted (black). See Fig. 3 for abbreviations and further details

frontal mechanisms, including cold, warm, and occluded fronts, as well as Gulf Lows and Nor'easters. There were no stationary fronts associated with precipitation during the study period. Most frontal precipitation events during the cool season were long in duration, with mean values >8 h (Table 6). Frontal precipitation events in this class were typically characterized by a strong center of low pressure to the northeast of the study area, coupled with troughing of 500 hPa heights, indicating the presence of cool moist air. These events were also sometimes associated with low pressure to the west of the study area coupled with some 500 hPa ridging near the study area, indicative of the presence of warmer and drier air. Cool season precipitation events associated with frontal mechanisms were significantly warmer than non-frontal precipitation events with significantly higher relative humidity and precipitation values (Table 2). Additionally, cool season frontal precipitation typically exhibited greater wind speeds and higher precipitation totals than precipitation events associated with warm season fronts (Table 2). During the cool season, precipitation intensities were greater during frontal events than during non-frontal precipitation events (Table 3).

Cold fronts accounted for ~27% of cool season frontal precipitation events (Table 6) and were associated with cool, moist air advected from the Gulf of Mexico (Fig. 5A). Warm fronts accounted for ~13% of cool season frontal precipitation events, and were

Table 6. Summary of cool season precipitation event types. Average total precipitation values are from National Weather Service cooperative observer (COOP) and Community Collaborative Rain, Hail, and Snow (CoCoRaHS) stations in the study area. Average temperature, relative humidity, wind speed, and wind direction are from the Beech Mountain (BEECHTOP) meteorological station. Significance: Levene = 0.004; Welch = 0.010

Event types	n	Mean spatial coverage (%)	Mean duration (range) (h)	Mean total precipitation (mm)	Temperature (°C)	Relative humidity (%)	Wind speed ($m\ s^{-1}$)	Wind direction (°)	Most frequent wind direction(s)	N	Monthly distribution (%) D	J	F	M	A
All frontal	48	73	16 (1–56)	16.1	–0.6	99.2	6.1	S (177)	SSE, NW	8	17	21	21	19	15
Cold front	13	70	8 (1–26)	10.0	0.1	99.1	4.1	W (273)	WNW	8		46		8	38
Warm front	6	76	15 (2–26)	17.6	4.1	100.0	13.1	SSE (161)	SSE	33			17	33	17
Occluded front	5	85	19 (8–31)	30.2	4.5	100.0	6.4	SSE (150)	SSE	20	20			60	
Gulf lows	19	74	20 (1–56)	19.1	–1.4	99.7	5.3	ESE (136)	SE, W	11	26	21	26	11	5
Nor'easters	5	59	18 (1 – 41)	4.8	–10.6	95.9	6.1	WNW (303)	WNW				80	20	
Non–frontal	12	52	17 (1–66)	3.6	–8.0	97.0	5.4	WNW (302)	NW			50	17	25	8

often influenced by air masses originating in the southeast (with moisture likely advected from the Atlantic Ocean) or northwest (Fig. 5B). These events were relatively warm compared to other cool season precipitation events (Table 6). Occluded fronts accounted for 10% of cool season frontal precipitation events and were the highest precipitation producers in this category, although the sample size was very small (n = 5) (Table 6). These events were associated with cool moist air from the west wedging below warmer and drier air from the east directly over the study area resulting in isentropic lifting and enhanced precipitation. Air masses typically originated off the Atlantic coast or to the northeast and approached the study area from the south (Fig. 5C). These events were the warmest of the cool season frontal precipitation events (Table 6) and exhibited the highest overall average precipitation intensity (Table 3).

Gulf Lows accounted for 40% of cool season frontal precipitation events and were relatively long in duration. These events were identified based on the absence of a clear frontal boundary within 300 km of the study area during maturation, while precipitation at the study area was connected to an area of low pressure over the Gulf of Mexico. These events were characterized by seasonably cool and moist air from the Gulf of Mexico encountering warmer and drier air from the east, inducing isentropic lifting and enhancing precipitation at the study area. Low-level airflow associated with these events originated over the Gulf of Mexico and also to the west and northwest of the study area (Fig. 5D). Nor'easters accounted for 10% of cool season frontal precipitation events and were identified by precipitation occurring in association with a well-defined surface low pressure passing near or to the northeast of the study area and in the absence of a clear frontal boundary within 300 km of the study area at event maturation. Air masses associated with these events typically originated to the west-northwest of the study area (Fig. 5E). Precipitation events associated with Nor'easters were the coldest of the cool season frontal precipitation events (Table 6).

Non-frontal events constituted ~20% of cool season precipitation events in this study. These event types took place in the absence of a clear frontal boundary within 300 km of the study area, and precipitation likely occurred as a result of upslope flow and orographic enhancement. This category is almost entirely characterized by low-level northwest upslope flow (Fig. 5F), 75% of which were snow events at the Boone AWOS (e.g. Perry et al. 2007).

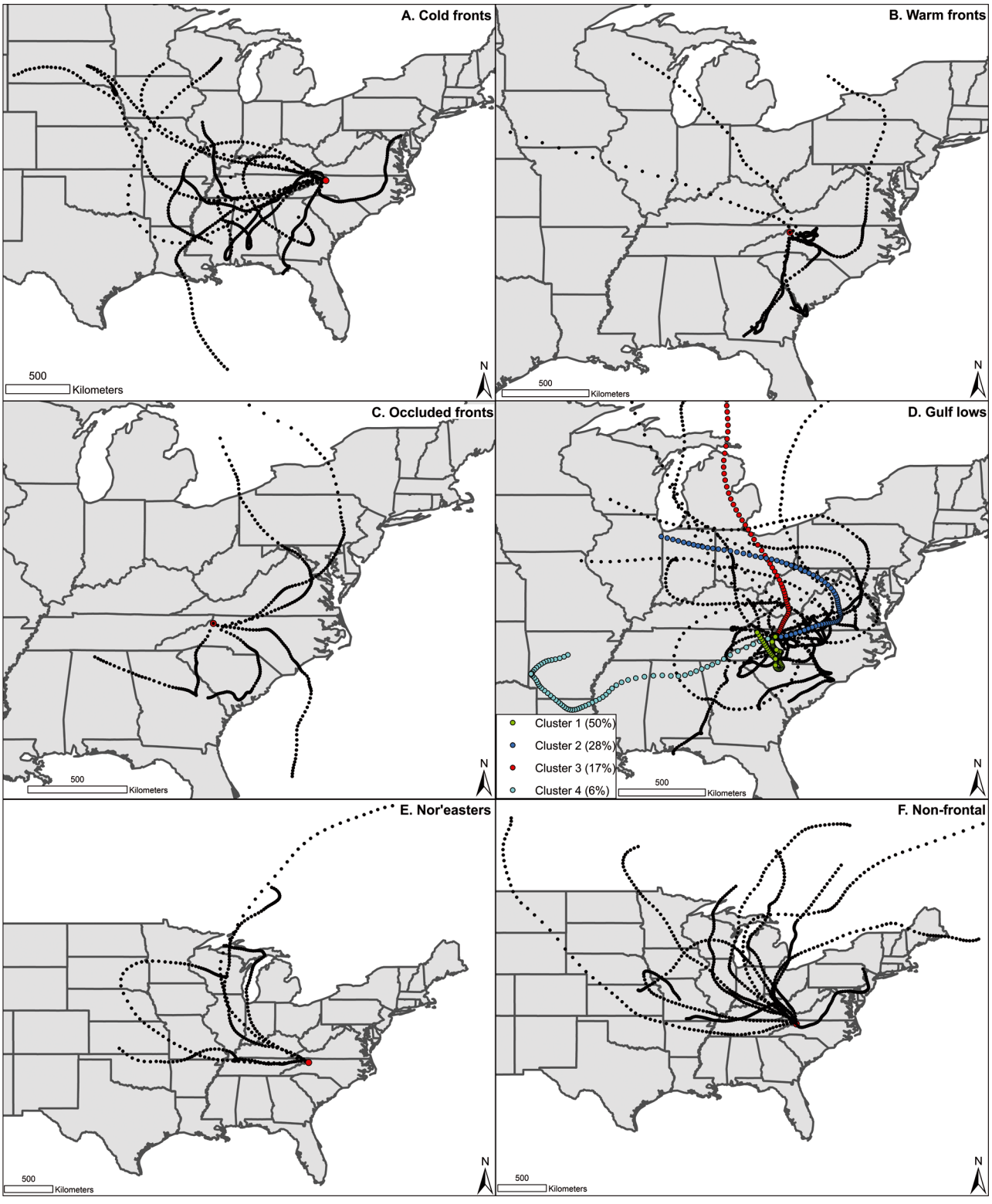

Fig. 5. Backward air trajectories representing maturation hour of each cool season precipitation event. Plots represent cool season precipitation events associated with (A) cold fronts, (B) warm fronts, (C) occluded fronts, (D) Gulf lows, (E) Nor'easters, and (F) non-frontal events. For cool season Gulf lows, HYbrid Single Particle Lagrangian Integrated Trajectory (HYSPLIT) cluster mean trajectories are shown in color; in all other cases, an insufficient number of backward air trajectories prevented cluster analysis: individual trajectories plotted instead (black)

West-to-east precipitation indices reveal very consistent patterns of precipitation during the cool season, particularly during cool season non-frontal precipitation, which was largely tied to NWFS (Table 5). Precipitation indices clearly demonstrate the orographic effects on precipitation for the antecedent air trajectory clusters, wherein Cluster 1 is the only cluster to come out of the east during the cool season (Fig. 3B) and it is the only cluster with a negative precipitation index value (i.e. less precipitation on western slopes). One-way ANOVA analysis results indicated statically significant differences in average precipitation among cool season frontal types (Levene = 0.004; Welch = 0.010) and cluster groups (Levene = 0.000; Welch = 0.036).

4. CONCLUSIONS

Our results highlight the importance of frontal boundaries to more widespread and heavier warm-season precipitation events during the study period. These findings may lend insight into future precipitation studies in the SAM, as well as in other mountainous regions.

Overall, frontal precipitation events in both seasons produced the highest amounts of precipitation during the period of this study, consistent with the findings of Keim (1996). Precipitation events during the warm season were characterized by short periods of heavy, intense precipitation. These precipitation events were likely associated with convective storms combined with weak upslope flow, that had overall greater spatial variability and less contrast in windward-leeward precipitation totals. Warm season frontal precipitation was strongly influenced by low-level air trajectories originating over the Gulf of Mexico and to the northwest, while non-frontal precipitation was strongly influenced by air masses that originated over coastal regions.

Cool season precipitation events were overall wetter and longer events, exhibiting less intense precipitation with pronounced spatial variability between windward and leeward slopes, particularly during cool season non-frontal precipitation (i.e. NWFS). Events associated with cool season occluded fronts exhibited the most intense precipitation as well as the highest precipitation totals. Air mass source regions influencing cool season frontal precipitation events primarily included inland areas to the north-northwest of the study area with a component originating near the Gulf of Mexico. Non-frontal precipitation during this season was dominated by NWFS.

Changes in atmospheric circulation patterns may lead to synoptic-scale conditions that affect precipitation patterns in the SAM. Summer (JJA) 2010 was one of the hottest periods on record for many regions in the SEUS, and it has been projected that the region may become drier and warmer in the coming decades (Karl et al. 2009, Li et al. 2010). Global circulation models (GCMs) forecast increased variability in precipitation patterns in the SEUS, indicating more intense periods of deluge and drought, particularly as a result of anthropogenic-induced warming (Li et al. 2010). Future research should include a longer term study period, to include hourly precipitation data from a larger number of stations within the study region. Our ongoing and planned future research activities include the investigation of synoptic patterns associated with precipitation in the SAM.

Acknowledgements. The authors gratefully acknowledge the many NWS COOP and CoCoRaHS precipitation observers, as well as the NOAA Air Resources Laboratory for the provision of the HYSPLIT transport and dispersion model (www.arl.noaa.gov/ready.php) used in this publication. C. Konrad offered advice in the design of the synoptic classification scheme, and D. Miller, J. Sherman, H. Neufeld, and R. Emanuel also offered helpful comments on the research design.

LITERATURE CITED

Barlow M, Nigam S, Berbery H (2001) ENSO, Pacific Decadal variability, and U.S. summertime precipitation, drought, and stream flow. J Clim 14:2105–2128

Barros AP, Kuligowski RJ (1998) Orographic effects during a severe wintertime rainstorm in the Appalachian Mountains. Mon Weather Rev 126:2648–2672

Barros AP, Lettenmaier DP (1994) Dynamic modeling of orographically induced precipitation. Rev Geophys 32: 265–284

Barry RG (2008) Mountain weather and climate. Cambridge University Press, Cambridge

Cifelli RN, Doesken N, Kennedy P, Carey LD, Rutledge SA, Gimmestad C, Depue T (2005) The Community Collaborative Rain, Hail, and Snow Network. Bull Am Meteorol Soc 86:1069–1077

Cortinas JV, Bernstein BC, Robbins CC, Strapp JW (2004) An analysis of freezing rain, freezing drizzle, and ice pellets across the United States and Canada: 1976-90. Weather Forecast 19:377–390

De Jong C, Lawler D, Essery R (2009) Mountain hydroclimatology and snow seasonality and hydrological change in mountain environments. Hydrol Processes 23:955–961

Diem JE (2006) Synoptic-scale controls of summer precipitation in the southeastern United States. J Clim 19:613–621

Draxler RR (1999) HYSPLIT4 user's guide. NOAA Tech Memo ERL ARL-230, NOAA Air Resources Laboratory, Silver Spring, MD

Draxler RR, Rolph GD (2011) HYSPLIT (HYbrid Single-Particle Lagrangian Integrated Trajectory). Model access via NOAA ARL READY Website, available at: http://ready.arl.noaa.gov/HYSPLIT.php (accessed 03 January)

Francou B, Vuille M, Wagnon P, Mendoza J, Sicart JE (2003) Tropical climate change recorded by a glacier in the central Andes during the last decades of the 20th century: Chacaltaya, Bolivia. J Geophys Res 108:D54154 doi: 10.1029/2002JD002959

Gaffin DM, Hotz DG (2000). A precipitation and flash flood climatology of the WFO Morristown hydrological service area. NOAA Tech Memo, NWS SR-204

Givati A, Rosenfeld D (2004) Quantifying precipitation suppression due to air pollution. J Appl Meteorol 43: 1038–1056

Graybeal DY, Leathers DJ (2006) Snowmelt-related flood risk in Appalachia: first estimates from a historical snow climatology. J Appl Meteorol Climatol 45:178–193

Harnack RK, Apffel K, Georgescu M, Baines S (2001) The determination of observed atmospheric differences between heavy and light precipitation events in New Jersey, USA. Int J Climatol 21:1529–1560

Jirak IL, Cotton WR (2006) Effect of air pollution on precipitation along the Front Range of the Rocky Mountains. J Appl Meteorol Climatol 45:236–245

Johnstone TP, Burrus SA (1998) An analysis of the 4 September 1996 Hickory Nut Gorge flash flood in western North Carolina. 16th Conf Weather Anal Forecast, Am Meteorol Soc 11-16 January 1998, Phoenix, AZ, p 275–277

Kalnay E, Kanamitsu M, Kistler R, Collins W, and others (1996) The NCEP/NCAR reanalysis 40-year project. Bull Am Meteorol Soc 77:437–471

Karl TR, Melillo JM, Peterson TC (2009) Global climate change impacts in the United States. Cambridge University Press, New York, NY

Kaser G, Hardy DR, Molg T (2004) Modern glacier retreat on Kilimanjaro as evidence of climate change: observations and facts. Int J Climatol 24:329–339

Keim BD (1996) Spatial, synoptic, and seasonal patterns of heavy rainfall in the southeastern United States. Phys Geogr 17:313–328

Kelly GM, Taubman BF, Perry LB, Sherman JP, Soulé PT, Sheridan PJ (in press) Relationships between aerosols and precipitation in the southern Appalachian Mountains. Int J Climatol

Konrad CE (1996) Relationships between precipitation event types and topography in the southern Blue Ridge Mountains of the Southeastern USA. Int J Climatol 16:49–62

Konrad CE (1997) Synoptic-scale features associated with warm season heavy rainfall over the interior southeastern United States. Weather Forecast 12:557–571

Konrad CE, Meentemeyer V (1994) Lower tropospheric warm air advection patterns associated with heavy rainfall over the Appalachian region. Prof Geogr 46:143–155

Lackmann G (2011) Midlatitude synoptic meteorology: dynamics, analysis, and forecasting. Am Meteor Soc, Boston, MA

Lapenta KD, McNaught BJ, Capriola SJ, Giordano LA and others (1995) The challenge of forecasting heavy rain and flooding throughout the Eastern Region of the National Weather Service. I. characteristics and events. Weather Forecast 10:78–90

Lecce SA (2000) Spatial variations in the timing of annual floods in the southeastern United States. J Hydrol (Amst) 235:151–169

Lee LG, Goodge GW (1984) Meteorological analysis of an intense 'east slope' rainstorm in the southern Appalachians. 10th Conf Weather Forecast Anal. Am Meteorol Soc, Boston, MA

Li W, Li L, Fu R, Deng Y, Wang H (2011) Changes to the North Atlantic subtropical high and its role in the intensification of summer rainfall variability in the southeastern United States. J Clim 24:1499–1506

Lin Y, Chiao S, Wang T, Kaplan ML, Weglarz RP (2001) Some common ingredients for heavy orographic rainfall. Weather Forecast 16:633–660

Lohmann U, Feichter J (2005) Global indirect aerosol effects: a review. Atmos Chem Phys 5:715–737

Lynn BH, Healy R, Druyan LM (2007) An analysis of the potential for extreme temperature change based on observations and model simulations. J Clim 20:1539–1554

Maddox RA, Chappell CF, Hoxit LR (1979) Synoptic and meso-α scale aspects of flash flood events. Bull Am Meteorol Soc 60:115–123

Maxwell JT, Soulé PT (2009) United States drought of 2007: historical perspectives. Clim Res 38:95–104

Miller JE (1946) Cyclogenesis in the Atlantic coastal region of the United States. J Meteorol 3:31–44

Mo KC, Schemm JE (2008) Relationships between ENSO and drought over the southeastern United States. Geophys Res Lett 35:L15701 10.1029/2008GL034656

Muller RA (1977) A synoptic climatology for environmental baseline analysis: New Orleans. J Appl Meteorol 16: 20–33

NCEP (2010a) National Climatic Data Center Service Records Retention System analysis and forecast charts. http://nomads.ncdc.noaa.gov/ncep/NCEP (accessed 12 January 2011)

NCEP (2010b) National Centers for Environmental Prediction daily weather maps. www.hpc.ncep.noaa.gov/dailywxmap/index.html (accessed 12 January 2011)

NCEP (2010c) National Oceanic and Atmospheric Administration Earth System Research Laboratory Daily mean composites. www.esrl.noaa.gov/psd/data/composites/day/ (accessed 12 January 2011)

Perry LB, Konrad CE (2006) Relationships between NW flow snowfall and topography in the Southern Appalachians, USA. Clim Res 32:35–47

Perry LB, Konrad CE, Schmidlin TW (2007) Antecedent upstream air trajectories associated with northwest flow snowfall in the Southern Appalachians. Weather Forecast 22:334–352

Perry LB, Hotz DG, Keighton SJ, Lee LG, Konrad CE, Dobson JG, Hall DK (2010) Overview of the 2009-2010 snow season in the southern Appalachian Mountains. 67th East Snow Conf, Hancock, MA

Power HC, Sheridan SC, Senkbeil JC (2006) Synoptic climatological influences on the spatial and temporal variability of aerosols over North America. Int J Climatol 26: 723–741

Rosenfeld D (1999) TRMM observed first direct evidence of smoke from forest fires inhibiting rainfall. Geophys Res Lett 26:3105–3108

Rosenfeld D, Dai J, Yu X, Yao Z, Xu X, Yang X (2007) Inverse relations between amounts of air pollution and orographic precipitation. Science 315:1396–1398

Sheridan SC (2002) The redevelopment of a weather-type classification scheme for North America. Int J Climatol 22:51–68

Taubman BF, Hains JD, Thompson AM, Marufu LT and others (2006) Aircraft vertical profiles of trace gas and aerosol pollution over the mid-Atlantic US: statistics and meteorological cluster analysis. J Geophys Res 111: D10S07 doi:10.1029/2005JD006196

Editorial responsibility: Oliver Frauenfeld, College Station, Texas, USA

Submitted: September 13, 2011; Accepted: June 7, 2012
Proofs received from author(s): October 19, 2012